Skeletal Muscle MiR-210 Expression is Associated with Mitochondrial Function in Peripheral Artery Disease Patients

Ahmed Ismaeel[a], **Emma Fletcher**[a], **Dimitrios Miserlis**[b], **Marissa Wechsler**[c], **Evlampia Papoutsi**[a], **Gleb Haynatzki**[d], **Robert S. Smith**[e], **William T. Bohannon, MD**[e], **Panagiotis Koutakis, PhD**[a,*]

[a]Department of Biology, Baylor University, Waco, TX, USA

[b]Department of Surgery, University of Texas Health Science Center San Antonio, San Antonio, TX, USA

[c]Department of Biomedical Engineering and Chemical Engineering, University of Texas at San Antonio, San Antonio, TX, USA

[d]Department of Biostatistics, University of Nebraska Medical Center, Omaha, NE

[e]Department of Surgery, Baylor Scott & White Medical Center, Temple, TX, USA

Abstract

Previous studies have demonstrated that circulating microRNA (miR)-210 levels are elevated in peripheral artery disease (PAD) patients. MiR-210 is known to be a negative regulator of mitochondrial respiration; however, the relationship between miR-210 and mitochondrial function has yet to be studied in PAD. We aimed to compare skeletal muscle miR-210 expression of PAD patients to non-PAD controls (CON) and to examine the relationship between miR-210 expression and mitochondrial function. Skeletal muscle biopsies from CON (n=20), intermittent claudication (IC) patients (n=20), and critical limb ischemia (CLI) patients (n=20) were analyzed by high-resolution respirometry to measure mitochondrial respiration of permeabilized fibers. Samples were also analyzed for miR-210 expression by real-time PCR. MiR-210 expression was significantly elevated in IC and CLI muscle compared to CON (p=0.008 and p<0.001, respectively). Mitochondrial respiration of electron transport chain (ETC) Complexes II (p=0.001) and IV (p<0.001) were significantly reduced in IC patients. Further, CLI patients demonstrated significant reductions in respiration during Complexes I (state 2: p=0.04, state 3: p=0.003), combined I and II (p<0.001), II (p<0.001), and IV (p<0.001). The expression of the miR-210 targets, cytochrome c oxidase assembly factor heme A:farnesyltransferase (COX10) and iron-sulfur cluster assembly enzyme (ISCU) were down-regulated in PAD muscle. MiR-210 may play

a role in the cellular adaptation to hypoxia and may be involved in the metabolic myopathy associated with PAD.

Keywords

electron transport chain; intermittent claudication; critical limb ischemia; revascularization; hypoxia

INTRODUCTION

Peripheral artery disease (PAD) most commonly presents as a result of atherosclerosis in the femoropopliteal or infrapopliteal arteries of the legs [1]. The main manifestation of the disease is intermittent claudication (IC), or exertion-induced pain or discomfort in the muscles distal to the occluded artery that is relieved by rest [1]. Less commonly, patients with the most advanced stage of PAD, critical limb ischemia (CLI), experience ischemic rest pain and ulcerations/gangrene [1]. PAD is associated with major reductions in walking performance, as well as accelerated decline of functional status over time [2].

Beyond altered hemodynamics due to arterial obstruction, other factors also play a role in the pathophysiological disabilities associated with PAD. One of the well-studied mechanisms believed to be linked to the exercise limitations in PAD is mitochondrial dysfunction [3]. Previous studies using high-resolution respirometry (the gold standard method to evaluate mitochondrial function) in permeabilized gastrocnemius myofibers have demonstrated reduced respiration in PAD muscle compared to non-PAD controls (CON) [4–6]. Furthermore, preclinical studies in murine hindlimb ischemia models support a causal role of mitochondrial dysfunction in PAD pathology, as different models of limb ischemia induced in mice by constriction or arterial ligation/excision result in impaired mitochondrial respiration as well [7–9].

One of the emerging factors that is increasingly being linked to regulation of mitochondrial function is post-transcriptional modulation by microRNAs (miRs) [10]. MiRs, endogenous noncoding RNAs ~21–25 nucleotides in length, are considered negative regulators of post-transcriptional gene expression, silencing mRNA molecules with complementary sequences by cleavage, destabilization, or reduced translation efficiency [10]. MiRs have also recently been studied as biomarkers in PAD patients [11–15]. For example, one miR that has been implicated in PAD is miR-210. Specifically, miR-210 expression was shown to be up-regulated in human atherosclerotic plaques [16], increased in PAD serum compared to CON, and inversely associated with pain-free walking distance [11, 15]. Interestingly, miR-210 is a target of Hypoxia-Inducible Factor 1-α (HIF1α), which directly activates miR-210 transcription under low oxygen tension, earning the miR its title as the "master hypoxamir" [17]. Activated miR-210 targets several transcripts involved in multiple aspects of cellular response to hypoxia, including repressing mitochondrial metabolism [18, 19]. *In vitro*, miR-210 was shown to decrease mitochondrial function and upregulate glycolysis by targeting and downregulating iron-sulfur cluster scaffold homolog (ISCU) and cytochrome *c* oxidase assembly protein (COX10) genes [20]. The iron sulfur clusters are major components of the ETC, and suppression of human ISCU inactivates mitochondrial enzymes

[21]. Furthermore, COX10 encodes a heme that is required for the expression of a functional cytochrome *c* oxidase protein, the terminal component of the ETC. COX10 deletion results in loss of Complex IV activity, and subsequent reductions in Complex I respiration [22].

Thus, in this study, we aimed to compare miR-210 expression in skeletal muscle tissue of PAD patients compared to CON and its association with mitochondrial function.

MATERIALS AND METHODS

Study Participants

Vascular surgeons at Baylor Scott and White Hospital and the University of Texas Health Science Center at San Antonio consecutively recruited 20 patients with symptomatic IC due to infrainguinal PAD. Additionally, 20 CLI patients with arterial insufficiency with gangrene, non-healing ischemic ulcers, or consistent rest pain, undergoing an amputation procedure were recruited. All diagnoses were made following physical and medical history examination, ankle brachial index (ABI) measurement, and arteriography. Twenty CON with normal blood flow to their extremities were also recruited. Patients with any musculoskeletal or neurologic symptoms, or acute lower extremity ischemic events secondary to thromboembolic disease or trauma, were excluded from the study. This study was approved by the Institutional Review Board of Baylor University under IRB Reference #1624041 and was carried out in accordance with relevant guidelines and regulations governing human research. The study complies with the Declaration of Helsinki, and informed consent was obtained from all participants.

Functional Assessment

The six-minute walk test was used to assess the total distance walked over the span of 6 minutes (6MWD) and pain-free walking time (PFWT) as indicators of lower extremity function in CON and IC patients. The 6-minute walk test was performed indoors in a long, flat, straight hallway. The walking course measured 15 m in length. The patient was asked to walk across the hallway to a turnaround point that was marked, turn around, and walk back. Patients were advised to achieve the greatest distance possible for six-minutes. The patients were asked to notify the tester of the first sign of claudication symptoms that develop. Each minute, the tester also called out the passing of the minute, along with a standardized encouragement phrase. Participants were allowed to rest during the test, but the 6-minute timer continued during the rest periods. Each lap was marked, and at the end of the test the patient was asked to stop walking. The additional distance walked from the last lap was measured with a measuring tape. The total distance walked was then calculated, rounding to the nearest meter. In CON patients, PFWT was associated with getting tired rather than exertional leg pain.

Muscle Biopsy and Blood Collection

Biopsies were obtained from the anteromedial segment of the gastrocnemius, approximately 10 cm distal to the tibial tuberosity. A fine needle (12G) was used to obtain a total sample of ~250 mg. Approximately 50 mg of the muscle was stored in ice-cold preservation solution

and immediately transferred to the lab for mitochondrial respiration measurements. Another 200 mg was snap-frozen in liquid nitrogen for later miR analysis.

Thirty mL of blood was obtained from each patient and control following an overnight fast. Blood was centrifuged (2000 g, 10 min, 4°C), and serum was aliquoted and stored at −80°C until time of analysis.

High-resolution Respirometry

Mitochondrial respiration in saponin-permeabilized muscle fibers was measured with an Oroboros O2k Oxygraph (Oroboros Instruments, Innsbruck, Austria). Respiration media consisted of 105 mM MES potassium salt, 30 mM potassium chloride (KCl), 10 mM potassium dihydrogen phosphate (KH_2PO_4), 5 mM magnesium chloride, hexahydrate ($MgCl_2.6H_2O$), and 0.5 mg/mL BSA. High-resolution oxygen consumption was measured at 25°C in a respiration buffer supplemented with creatine monohydrate (20 mM). A substrate inhibitor titration protocol was performed, in which 2 mM malate and 10 mM glutamate were added to the chambers to measure Complex I, state 2 respiration. This was followed by 4 mM ADP addition, to initiate state 3 (ADP-stimulated) respiration. Next, 10 mM succinate was added to the chambers to stimulate electron flow through Complex II as well. Rotenone (10 μM) was used to inhibit Complex I, and 10 μM cytochrome c was added to test the mitochondrial membrane integrity. Finally, Complex IV respiration was determined using 0.4 mM *N,N,N',N'*-tetramethyl-*p*-phenylenediamine (TMPD), 2 mM ascorbate to prevent TMPD auto-oxidation, and 5 μM antimycin A to inhibit electron flow through Complex III. All reagents and chemicals were purchased from Sigma Aldrich (St. Louis, MO). A Pierce BCA Protein Assay Kit (Thermo Fisher Scientific, Waltham, MA, 23225) was used to measure protein concentrations, and the respiration rate was expressed as pmol oxygen consumed per second, normalized to protein content (pmols/s/μg protein).

Citrate Synthase Assay

A commercial Citrate Synthase Assay Kit (Sigma Aldrich, CS0720) was used to measure citrate synthase (CS) activity in skeletal muscle lysates as a measure of mitochondrial content. Specifically, CS activity was determined colorimetrically using the substrate 5,5'-Dithiobis-(2-nitrobenzoic acid) (DTNB) (10mM). A reaction mix containing the DTNB substrate, muscle lysate (8 μg protein), 30 mM acetyl coenzyme A (CoA) and 10mM oxaloacetic acid (OAA) was prepared for all samples. In the presence of OAA, CS catalyzes the reaction between a thiol group of acetyl CoA and DTNB to produce 5-thio-2-nitrobenzoic acid (TNB). Thus, CS activity was measured by monitoring the change in absorbance (i.e., TNB formation) every 10 seconds for 5 min (25°C) (Varioskan LUX microplate reader, Waltham, MA) in 96 well plates. All samples were assayed in duplicate at a wavelength of 412 nm with blank values subtracted.

MiR-210 and miR-210 Targets

The RNeasy Mini Kit (74104, Qiagen, Hilden, Germany) and miRNeasy Mini Kit (Qiagen, 217084) were used to purify total RNA and miR from gastrocnemius tissue homogenates. The Quick-cfRNA Serum & Plasma Kit (Zymo Research, Irvine, CA, R1059) was used to isolate miR from serum samples. A Taqman® Advanced miRNA cDNA Synthesis Kit

(Applied Biosystems, Waltham, MA, A28007) was used to prepare cDNA templates for miR assays. MiR-210 gene expression was analyzed by real-time PCR using a Taqman® Advanced miRNA Assay kit (Applied Biosystems, A25576) run on a QuantStudio™ 6 PCR system (Applied Biosystems). The following miR-210 primer was used: hsa-miR-210-3p, mature miR sequence 5'-CUGUGCGUGUGACAGCGGCUGA-3' (Applied Biosystems, 477970_mir). Threshold cycle (C_T) values between miR-210 and the endogenous control U6B small nuclear RNA (RNU6B) (Thermo Fisher Scientific, 001093) gene was used to normalize data [23]. The 2^ (-delta delta C_T) method was used to calculate fold change.

To determine the relative expression of miR-210 target genes by PCR array, a RT^2 First Strand Kit (Qiagen, 330401) was used for cDNA synthesis, and the cDNA was used on the real-time RT^2 Profiler PCR Array PAHS-6009Z (Qiagen, 330231) in combination with RT^2 SYBR® Green qPCR Mastermix (Qiagen, 330513), run on a QuantStudio™ 6 PCR system. Data was uploaded to GeneGlobe (Qiagen) for analysis, using the delta delta C_T method between genes of interest, normalized with the geometric mean of reference housekeeping genes (ACTB, B2M, GAPDH, HPRT1, RPLP0).

To determine the relative gene expression of COX10 and ISCU by real-time PCR, total RNA was isolated from gastrocnemius samples using the Direct-zol RNA Microprep kit (R2062, Zymo Research), and then cDNA was synthesized using an iScript Advanced cDNA synthesis Kit (Bio-Rad Laboratories, Hercules, CA, 1725037). PCR reactions used the following primers: COX10 (Integrated DNA Technologies, Coralville, IA, Hs.PT.58.600173), ISCU (Integrated DNA Technologies, Hs.PT.58.3372427), and the housekeeping genes GAPDH (Integrated DNA Technologies, Hs.PT.39a.22214836) and ACTB (Integrated DNA Technologies, Hs.PT.39a.22214847), at a final concentration of 250 nM and 1x PrimeTime Gene Expression Master Mix (Integrated DNA Technologies, 1055770), run on a CFX Opus Real-Time PCR System (Bio-Rad Laboratories). Table 1 lists the primer pair sequences. The quantification cycle (Cq) of target genes was normalized to the reference genes (GAPDH and ACTB), and relative normalized expression was calculated using the 2^(-delta delta Cq) method. All samples were run in triplicate, and results were averaged.

For protein expression analysis by western blotting, muscles were first homogenized in lysis buffer consisting of 50 mM Tris-HCl, 150 mM NaCl, 1% NP-40, 0.25% sodium-deoxycholate, 0.1% SDS, and 1x protease inhibitor cocktail (Sigma Aldrich, P8340) for protein isolation. Protein samples were subsequently mixed with premixed 4x Laemmli protein sample buffer (Bio-Rad Laboratories, 1610747) and 2-mercaptoethanol reducing agent (Bio-Rad Laboratories, 1610710). Using 4–20% Criterion TGX Precast Midi Protein Gels (Bio-Rad Laboratories, 5671095), 20 μg of protein were separated using electrophoresis in a Criterion Cell Tank (Bio-Rad Laboratories). Proteins were transferred to 0.2 μm Amersham Hybond P polyvinylidene difluoride (PVDF) transfer membranes (Cytiva, Malborough, MA, 10600021) and incubated in primary antibodies (COX10 (1:1000): ProteinTech, Rosemont, IL, 10611; ISCU (1:1000): ProteinTech, 14812; GAPDH (1:10,000): Protein Tech, 10494) for 90 min at room temperature. Following, membranes were incubated with appropriate HRP-conjugated secondary antibody (Goat anti-Rabbit IgG (H+L) (1:10,000), Invitrogen, Waltham, MA, 31462). Membranes were visualized using

Clarity ECL Substrate (Bio-Rad Laboratories, 1705060), and bands were detected using the ChemiDoc MP Imaging System (Bio-Rad Laboratories). Band intensities were quantified using Image Lab (Bio-Rad Laboratories), and protein levels were expressed as fold changes of the protein adjusted to the loading control, GAPDH, relative to the CON group.

Statistics

Patient demographics and clinical characteristics were compared using analysis of variance (ANOVA) for continuous variables and chi-square and Fisher exact tests for categorical variables. A one-way analysis of covariance (ANCOVA) was used to test differences in miR-210 expression, expression of miR-210 targets, and mitochondrial respiration between CON, IC, and CLI groups, adjusting for significant covariates. An independent samples t-test was also used to test the difference in miR-210 expression between males and females. The assumptions of normality and homogeneity of variances were verified prior to analyses. Equal variances were verified using descriptives and Levene's test. For ANCOVA tests, post-hoc analyses were performed with Bonferroni correction. Additionally, Pearson correlations were calculated to test the association between miR-210 expression and 6MWD, PFWT, and complex-specific mitochondrial respiration. A Pearson correlation was also calculated to test the association between circulating and muscle miR-210 levels. All analyses were performed using SPSS statistical software version 25 (IBM, Armonk, NY, USA). Significance was set at α 0.05. Sample size analysis (G*Power [24]), calculated using reported data on detecting changes in miR-210 expression in PAD patients [11, 15] (primary outcome), indicated that 8 patients per group provides adequate study power (1-β = 0.8).

Data Availability: The datasets generated during and/or analyzed during the current study are available from the corresponding author on reasonable request.

RESULTS

Clinical Characteristics

The participant demographics and clinical characteristics are presented in Table 2. As expected, ABI values were higher in CON compared to both IC patients and CLI patients ($p<0.001$). Additionally, 6MWD and PFWT were also significantly lower in IC patients compared to CON ($p<0.001$ for both).

Mitochondrial Function

The oxygen consumption rate was significantly lower in permeabilized muscle fibers from IC patients and CLI patients during Complex II respiration (CII) ($p=0.001$ and $p<0.001$, respectively) and Complex IV respiration (CIV) ($p<0.001$ for both), relative to CON muscle (Figure 1). CLI patients demonstrated further reductions in respiration during Complex I, state 2 (CI.2) ($p=0.04$), Complex I, state 3 (CI.3) ($p=0.003$), and combined Complex I and II (CI+II) respiration ($p<0.001$). CS activity was not different between groups ($p=0.64$), suggesting similar mitochondrial content across samples (Figure 1F).

MiR-210 and miR-210 Target Expression

Gastrocnemius miR-210 expression was significantly higher in IC and CLI patients relative to CON (1.69 ± 0.64-fold, p=0.008 and 2.12 ± 0.49-fold, p<0.001, respectively) (Figure 2A). Although miR-210 levels were higher in CLI patients compared to IC, the difference was not statistically significant (p=0.15). Since the CON group included more females, we assessed for biological sex differences within groups in miR-210 expression. There were no significant differences in miR-210 expression between male and female patients in any of the groups (CON male: 0.97 ± 0.27-fold, CON female: 1.07 ± 0.26-fold, p=0.65; IC male: 1.69 ± 0.64-fold, IC female: 1.67 ± 0.16-fold, p=0.95; CLI male: 2.23 ± 0.41-fold, CLI female: 2.04 ± 48-fold, p=0.85).

Circulating levels of miR-210 were also significantly higher in IC and CLI patients relative to CON (1.53 ± 0.16-fold, p=0.003 and 2.23 ± 0.38-fold, p<0.001, respectively) (Figure 2B). Furthermore, circulating levels of miR-210 were significantly higher in CLI patients compared to IC patients as well (p<0.001). Skeletal muscle expression of miR-210 correlated significantly with circulating miR-210 levels (R^2=0.67, p<0.001) (Figure 2C). Interestingly, skeletal muscle miR-210 expression significantly correlated with CI+II (R^2=0.33, p=0.001), and CIV respiration (R^2=0.28, p=0.004) (Figure 3A–B). Furthermore, miR-210 levels also significantly correlated with 6MWD (R^2=0.45, p=0.001) (Figure 3C), but not with PFWT (p=0.54).

The PCR array of miR-210 targets identified the following differentially expressed genes in IC muscle (n=6) relative to CON (n=3): COX10 (p=0.005), glycerol-3-phosphate dehydrogenase 1 like (GPD1L) (p<0.001), ISCU (p<0.001), Clustered Mitochondria Homolog (CLUH) (p=0.02), Lysosomal Associated Membrane Protein 1 (LAMP1) (p<0.001), MID1 Interacting Protein 1 (MID1IP1) (p<0.001), NADH Dehydrogenase 1 Alpha Subcomplex 4 (NDUFA4) (p<0.001), and Zinc Finger AN1-Type Containing 3 (ZFAND3) (p<0.001).

COX10 (p=0.003), GPD1L (p<0.001), ISCU (p<0.001), NDUFA4 (p=0.01), and ZFAND3 (p=0.002), were also differentially expressed in CLI tissue (n=3) relative to CON, along with Cholinergic Receptor Nicotinic Beta 1 Subunit (CHRNB1) (p=0.02). The complete list of the miR-210 targets assessed by the PCR array is presented in Figure 4, and the complete PCR array data are provided in Supplementary Table 1.

To confirm the PCR array results for COX10 and ISCU, we determined the mRNA levels of these genes in a larger sample of CON (n=10), IC (n=10), and CLI patients (n=10). The gastrocnemius mRNA expression of both COX10 and ISCU were significantly down-regulated in IC patients (COX10: 0.53 ± 0.30-fold, p=0.01; ISCU: 0.42 ± 0.37-fold, p<0.001) relative to CON (Figure 5A). In CLI patients, ISCU was significantly down-regulated (0.35 ± 0.13-fold, p<0.001), and although COX10 levels trended towards down-regulation (0.71 ± 0.40-fold, p=0.15), differences were not statistically significant relative to CON. The protein expression of COX10 and ISCU was also significantly lower in IC (0.23 ± 0.23-fold, p=0.01 and 0.44 ± 0.36-fold, p=0.01, respectively) and CLI (0.37 ± 0.36-fold, p=0.04 and 0.52 ± 0.31, p=0.049, respectively) compared to CON (Figure 5B,C).

DISCUSSION

The human genome codes for over 1000 miRs, and a third of all mRNAs may be targeted by miRs [25]. Since miRs can affect cellular and physiological processes, miR levels have been studied in the context of different pathological processes. With relevance to atherosclerosis, five different miRs have been found to be upregulated in human atherosclerotic plaque, compared to non-atherosclerotic arteries [16]. Of these, miR-210 was also shown to be significantly increased in serum samples of PAD patients in two studies [11, 15]. Here, we corroborate these findings and show that miR-210 is also elevated in ischemic muscle of PAD patients. Additionally, Signorelli et al. showed that miR-210 levels inversely correlated with PFWD [11], and in our study we demonstrate a negative association between skeletal muscle miR-210 and 6MWD. Taken together, these results suggest that miR-210 may represent a potential biomarker for the diagnosis and prognosis of PAD.

MiR-210 may be especially important in ischemic conditions due to its induction by HIF-1α during hypoxia [26] (Figure 6). In fact, HIF-1α directly binds to a hypoxia response element (HRE) on the proximal miR-210 promoter [27]. The HRE is located upstream of miR-210's transcription start site, which suggests that the HRE is responsible for hypoxic induction of pri-miR-210 [27]. Interestingly, the HRE site on the miR-210 promoter region is also highly conserved across species, further exemplifying the role of hypoxia in miR-210 expression. Other transcriptional factor binding sites that are also highly conserved that are located in close proximity to miR-210's HRE site include transcription factors involved in energy metabolism, such as E2F1 and peroxisome proliferator-activated receptor-γ [27]. This observation is consistent with the importance of hypoxia in the regulation of energy metabolism. Due to a limited oxygen supply, hypoxia suppress mitochondrial energy metabolism, and this process is known to involve induction of several proteins including pyruvate dehydrogenase kinase, lactate dehydrogenase A, and COX4–10 [28]. Recent evidence suggests that miR-210 induction may also play a role in the cellular energy production shift under hypoxia. Mechanistically, this occurs via repression of ISCU and COX10 [20]. Thus, since the identification of the HIF-1α/miR-210/ISCU-COX10 regulatory axis, this axis has been studied in several conditions ranging from cancer and ischemic heart disease to preeclampsia [29–31]. Notably, other potential targets of miR-210 have also been identified that may further explain miR-210-mediated reductions in mitochondrial activity, including Succinate Dehydrogenase Complex Subunit D (SDHD) [31, 32] and NADH dehydrogenase ubiquinone 1 alpha subcomplex 4 (NDUFA4) [33]. Several studies have shown that miR-210 is sufficient to reduce Complex I [18, 29, 34], Complex II [32, 35–37], and Complex IV [29, 33] activity. Interestingly, our work also demonstrated negative associations between miR-210 expression and Complex I+II, and Complex IV respiration.

One of the well-studied features of PAD is an associated skeletal muscle metabolic myopathy that is characterized by histological alterations as well as mitochondrial dysfunction [3]. One of the primary treatment goals for PAD patients is to improve walking performance, and targeting the mitochondria is recognized as a promising approach. Recently, two studies by Gratl et al. showed improvements in mitochondrial function by interventional revascularization of arteriosclerotic lesions [38, 39]. These studies suggest an underlying mechanism of improved mitochondrial performance related to re-established

blood and oxygen supply. Thus, recovered mitochondrial respiration after successful invasive revascularization for PAD may involve normalization of miR-210 levels. Future studies should assess the effect of different interventions that improve mitochondrial function and walking performance, such as surgical revascularization, on miR-210 levels in PAD patients.

One important noteworthy point is that in addition to the effects on mitochondrial respiration, miR-210 may also play a role in other biological mechanisms relevant to PAD. For example, miR-210 has been studied in the context of acute hindlimb ischemia (HLI) in mice, where miR-210 overexpression has been shown to improve angiogenesis and blood perfusion recovery and increase arteriolar and capillary density [40–42]. These effects are thought to result via miR-210-mediated inhibition of ephrin A3 [43] and protein tyrosine phosphatase 1B [44]. In other preclinical studies, increasing miR-210 levels in endothelial cells has also been shown to protect against hypoxia/reoxygenation injury by reducing reactive oxygen species (ROS) production [45]. Likewise, in acute HLI models, miR-210 overexpression has been found to decrease ROS production, and miR-210 antagonism was shown to increase oxidative stress [42, 46]. However, the effects of miR-210 have yet to be studied under chronic hypoxia, which emphasizes the importance of further investigations into miR-210 using prolonged, *in-vitro* and *in-vivo* ischemia models.

The role of miR-210 in human PAD remains unclear. While the present identified inverse associations between miR-210 expression and mitochondrial respiration in PAD, these findings are only correlational. Importantly, miR-210 up-regulation in PAD may play a role in cellular adaptation to hypoxia and may represent a mechanism for protection against low oxygen conditions. Thus, a limitation of this work is the descriptive nature of the study, and therefore, cause and effect linkages between miR-210 and mitochondrial dysfunction in PAD cannot be established. Future studies should confirm and further analyze these associations in preclinical models. Further, the sample size of the study was relatively small, so external validation from a larger sample may improve the translational impact of the study results.

In conclusion, miR-210 may represent a potential novel biomarker for the diagnosis and prognosis of PAD and a start point for individualized treatment. Our findings warrant future studies to understand the role of miR-210 in regulating mitochondrial and oxidative metabolism across the spectrum of the disease.

Supplementary Material

Refer to Web version on PubMed Central for supplementary material.

Acknowledgements:

Author Manuscript

Financial support:

Abbreviations:

PAD	Peripheral artery disease
IC	intermittent claudication
CLI	critical limb ischemia
miR	micro-RNA
ISCU	iron-sulfur cluster assembly enzyme
COX10	cytochrome c oxidase assembly factor heme A:farnesyltransferase
ABI	ankle brachial index
6MWD	6-minute walk distance
PFWT	pain-free walking time
JO2	oxygen flux

References

[1]. Chen Q, Smith CY, Bailey KR, Wennberg PW, Kullo IJ. Disease Location Is Associated With Survival in Patients With Peripheral Arterial Disease. 2013.

[2]. McDermott MM, Liu K, Greenland P, Guralnik JM, Criqui MH, Chan C, et al. Functional decline in peripheral arterial disease: associations with the ankle brachial index and leg symptoms. Jama. 2004;292:453–61. [PubMed: 15280343]

[3]. Kim K, Anderson EM, Scali ST, Ryan TE. Skeletal Muscle Mitochondrial Dysfunction and Oxidative Stress in Peripheral Arterial Disease: A Unifying Mechanism and Therapeutic Target. Antioxidants (Basel). 2020;9.

[4]. Koutakis P, Miserlis D, Myers SA, Kim JK, Zhu Z, Papoutsi E, et al. Abnormal accumulation of desmin in gastrocnemius myofibers of patients with peripheral artery disease: associations with altered myofiber morphology and density, mitochondrial dysfunction and impaired limb function. J Histochem Cytochem. 2015;63:256–69. [PubMed: 25575565]

[5]. Pipinos II, Sharov VG, Shepard AD, Anagnostopoulos PV, Katsamouris A, Todor A, et al. Abnormal mitochondrial respiration in skeletal muscle in patients with peripheral arterial disease. J Vasc Surg. 2003;38:827–32. [PubMed: 14560237]

[6]. Pipinos II, Judge AR, Zhu Z, Selsby JT, Swanson SA, Johanning JM, et al. Mitochondrial defects and oxidative damage in patients with peripheral arterial disease. Free Radic Biol Med. 2006;41:262–9. [PubMed: 16814106]

[7]. Pipinos II, Swanson SA, Zhu Z, Nella AA, Weiss DJ, Gutti TL, et al. Chronically ischemic mouse skeletal muscle exhibits myopathy in association with mitochondrial dysfunction and oxidative damage. Am J Physiol Regul Integr Comp Physiol. 2008;295:R290–6. [PubMed: 18480238]

[8]. Ryan TE, Schmidt CA, Tarpey MD, Amorese AJ, Yamaguchi DJ, Goldberg EJ, et al. PFKFB3-mediated glycolysis rescues myopathic outcomes in the ischemic limb. JCI Insight. 2020;5.

[9]. Schmidt CA, Ryan TE, Lin CT, Inigo MMR, Green TD, Brault JJ, et al. Diminished force production and mitochondrial respiratory deficits are strain-dependent myopathies of subacute limb ischemia. J Vasc Surg. 2017;65:1504–14 e11. [PubMed: 28024849]

[10]. Li P, Jiao J, Gao G, Prabhakar BS. Control of mitochondrial activity by miRNAs. J Cell Biochem. 2012;113:1104–10. [PubMed: 22135235]

[11]. Signorelli SS, Volsi GL, Pitruzzella A, Fiore V, Mangiafico M, Vanella L, et al. Circulating miR-130a, miR-27b, and miR-210 in Patients With Peripheral Artery Disease and Their Potential Relationship With Oxidative Stress. Angiology. 2016;67:945–50. [PubMed: 26980776]

[12]. Bogucka-Kocka A, Zalewski DP, Ruszel KP, Stepniewski A, Galkowski D, Bogucki J, et al. Dysregulation of MicroRNA Regulatory Network in Lower Extremities Arterial Disease. Front Genet. 2019;10:1200. [PubMed: 31827490]

[13]. Zhou X, Yuan P, He Y. Role of microRNAs in peripheral artery disease (review). Mol Med Rep. 2012;6:695–700. [PubMed: 22767222]

[14]. Syed MH, Zamzam A, Valencia J, Khan H, Jain S, Singh KK, et al. MicroRNA Profile of Patients with Chronic Limb-Threatening Ischemia. Diagnostics (Basel). 2020;10.

[15]. Li TR, Cao HC, Zhuang JM, Wan J, Guan M, Yu B, et al. Identification of miR-130a, miR-27b and miR-210 as serum biomarkers for atherosclerosis obliterans. Clin Chim Acta. 2011;412:66–70. [PubMed: 20888330]

[16]. Raitoharju E, Lyytikainen LP, Levula M, Oksala N, Mennander A, Tarkka M, et al. miR-21, miR-210, miR-34a, and miR-146a/b are up-regulated in human atherosclerotic plaques in the Tampere Vascular Study. Atherosclerosis. 2011;219:211–7. [PubMed: 21820659]

[17]. Chan YC, Banerjee J, Choi SY, Sen CK. miR-210: the master hypoxamir. Microcirculation. 2012;19:215–23. [PubMed: 22171547]

[18]. Chan SY, Zhang YY, Hemann C, Mahoney CE, Zweier JL, Loscalzo J. MicroRNA-210 controls mitochondrial metabolism during hypoxia by repressing the iron-sulfur cluster assembly proteins ISCU1/2. Cell Metab. 2009;10:273–84. [PubMed: 19808020]

[19]. Favaro E, Ramachandran A, McCormick R, Gee H, Blancher C, Crosby M, et al. MicroRNA-210 regulates mitochondrial free radical response to hypoxia and krebs cycle in cancer cells by targeting iron sulfur cluster protein ISCU. PLoS One. 2010;5:e10345. [PubMed: 20436681]

[20]. Chen Z, Li Y, Zhang H, Huang P, Luthra R. Hypoxia-regulated microRNA-210 modulates mitochondrial function and decreases ISCU and COX10 expression. Oncogene. 2010;29:4362–8. [PubMed: 20498629]

[21]. Tong WH, Rouault TA. Functions of mitochondrial ISCU and cytosolic ISCU in mammalian iron-sulfur cluster biogenesis and iron homeostasis. Cell Metab. 2006;3:199–210. [PubMed: 16517407]

[22]. Diaz F, Fukui H, Garcia S, Moraes CT. Cytochrome c oxidase is required for the assembly/stability of respiratory complex I in mouse fibroblasts. Mol Cell Biol. 2006;26:4872–81. [PubMed: 16782876]

[23]. Das MK, Andreassen R, Haugen TB, Furu K. Identification of Endogenous Controls for Use in miRNA Quantification in Human Cancer Cell Lines. Cancer Genom Proteom. 2016;13:63–8.

[24]. Faul F, Erdfelder E, Buchner A, Lang AG. Statistical power analyses using G*Power 3.1: Tests for correlation and regression analyses. Behav Res Methods. 2009;41:1149–60. [PubMed: 19897823]

[25]. Kozomara A, Birgaoanu M, Griffiths-Jones S. miRBase: from microRNA sequences to function. Nucleic Acids Res. 2019;47:D155–D62. [PubMed: 30423142]

[26]. Crosby ME, Kulshreshtha R, Ivan M, Glazer PM. MicroRNA regulation of DNA repair gene expression in hypoxic stress. Cancer Res. 2009;69:1221–9. [PubMed: 19141645]

[27]. Huang X, Ding L, Bennewith KL, Tong RT, Welford SM, Ang KK, et al. Hypoxia-inducible mir-210 regulates normoxic gene expression involved in tumor initiation. Molecular cell. 2009;35:856–67. [PubMed: 19782034]

[28]. Semenza GL. Oxygen-dependent regulation of mitochondrial respiration by hypoxia-inducible factor 1. Biochem J. 2007;405:1–9. [PubMed: 17555402]

[29]. Muralimanoharan S, Maloyan A, Mele J, Guo C, Myatt LG, Myatt L. MIR-210 modulates mitochondrial respiration in placenta with preeclampsia. Placenta. 2012;33:816–23. [PubMed: 22840297]

[30]. Hu SJ, Huang M, Li ZJ, Jia FJ, Ghosh ZM, Lijkwan MA, et al. MicroRNA-210 as a Novel Therapy for Treatment of Ischemic Heart Disease. Circulation. 2010;122:S124–S31. [PubMed: 20837903]

[31]. Dang K, Myers KA. The role of hypoxia-induced miR-210 in cancer progression. Int J Mol Sci. 2015;16:6353–72. [PubMed: 25809609]

[32]. Puissegur MP, Mazure NM, Bertero T, Pradelli L, Grosso S, Robbe-Sermesant K, et al. miR-210 is overexpressed in late stages of lung cancer and mediates mitochondrial alterations associated with modulation of HIF-1 activity. Cell Death Differ. 2011;18:465–78. [PubMed: 20885442]

[33]. Tian F, Tang P, Sun Z, Zhang R, Zhu D, He J, et al. miR-210 in Exosomes Derived from Macrophages under High Glucose Promotes Mouse Diabetic Obesity Pathogenesis by Suppressing NDUFA4 Expression. J Diabetes Res. 2020;2020:6894684. [PubMed: 32258168]

[34]. Sun W, Zhao L, Song X, Zhang J, Xing Y, Liu N, et al. MicroRNA-210 Modulates the Cellular Energy Metabolism Shift During H2O2-Induced Oxidative Stress by Repressing ISCU in H9c2 Cardiomyocytes. Cell Physiol Biochem. 2017;43:383–94. [PubMed: 29032377]

[35]. Anton L, DeVine A, Polyak E, Olarerin-George A, Brown AG, Falk MJ, et al. HIF-1alpha Stabilization Increases miR-210 Eliciting First Trimester Extravillous Trophoblast Mitochondrial Dysfunction. Front Physiol. 2019;10:699. [PubMed: 31263422]

[36]. Voloboueva LA, Sun X, Xu L, Ouyang YB, Giffard RG. Distinct Effects of miR-210 Reduction on Neurogenesis: Increased Neuronal Survival of Inflammation But Reduced Proliferation Associated with Mitochondrial Enhancement. J Neurosci. 2017;37:3072–84. [PubMed: 28188219]

[37]. Grosso S, Doyen J, Parks SK, Bertero T, Paye A, Cardinaud B, et al. MiR-210 promotes a hypoxic phenotype and increases radioresistance in human lung cancer cell lines. Cell Death Dis. 2013;4.

[38]. Gratl A, Frese J, Speichinger F, Pesta D, Frech A, Omran S, et al. Regeneration of Mitochondrial Function in Gastrocnemius Muscle in Peripheral Arterial Disease After Successful Revascularisation. Eur J Vasc Endovasc Surg. 2020;59:109–15. [PubMed: 31786105]

[39]. Gratl A, Pesta D, Gruber L, Speichinger F, Raude B, Omran S, et al. The effect of revascularization on recovery of mitochondrial respiration in peripheral artery disease: a case control study. J Transl Med. 2021;19:244. [PubMed: 34088309]

[40]. Zaccagnini G, Maimone B, Fuschi P, Longo M, Da Silva D, Carrara M, et al. Hypoxia-Induced miR-210 Is Necessary for Vascular Regeneration upon Acute Limb Ischemia. Int J Mol Sci. 2019;21.

[41]. Zaccagnini G, Maimone B, Fuschi P, Maselli D, Spinetti G, Gaetano C, et al. Overexpression of miR-210 and its significance in ischemic tissue damage. Sci Rep. 2017;7:9563. [PubMed: 28842599]

[42]. Zaccagnini G, Maimone B, Di Stefano V, Fasanaro P, Greco S, Perfetti A, et al. Hypoxia-induced miR-210 modulates tissue response to acute peripheral ischemia. Antioxid Redox Signal. 2014;21:1177–88. [PubMed: 23931770]

[43]. Fasanaro P, D'Alessandra Y, Di Stefano V, Melchionna R, Romani S, Pompilio G, et al. MicroRNA-210 modulates endothelial cell response to hypoxia and inhibits the receptor tyrosine kinase ligand Ephrin-A3. J Biol Chem. 2008;283:15878–83. [PubMed: 18417479]

[44]. Fasanaro P, Greco S, Lorenzi M, Pescatori M, Brioschi M, Kulshreshtha R, et al. An integrated approach for experimental target identification of hypoxia-induced miR-210. J Biol Chem. 2009;284:35134–43. [PubMed: 19826008]

[45]. Ma X, Wang J, Li J, Ma C, Chen S, Lei W, et al. Loading MiR-210 in Endothelial Progenitor Cells Derived Exosomes Boosts Their Beneficial Effects on Hypoxia/Reoxygeneation-Injured Human Endothelial Cells via Protecting Mitochondrial Function. Cell Physiol Biochem. 2018;46:664–75. [PubMed: 29621777]

[46]. Zhang JF, Rao GT, Qiu JY, He RH, Wang QT. MicroRNA-210 improves perfusion recovery following hindlimb ischemia via suppressing reactive oxygen species. Exp Ther Med. 2020;20.

Author Manuscript

Author Manuscript

Author Manuscript

Author Manuscript

Brief Commentary

Background:

Peripheral artery disease (PAD) is characterized by a metabolic myopathy, and mitochondrial dysfunction significantly contributes to PAD pathophysiology. MicroRNA-210 (MiR-210) has been identified as a negative regulator of mitochondrial respiration during hypoxia. We compared skeletal muscle miR-210 expression of PAD patients to non-PAD controls and examined the relationship between miR-210 and mitochondrial function.

Translational Significance:

MiR-210 levels were increased in PAD patients and negatively associated with mitochondrial respiration and walking performance. MiR-210 may play a role in cellular adaptation to hypoxia in PAD. Future studies should clarify the role of miR-210 in the metabolic myopathy associated with PAD.
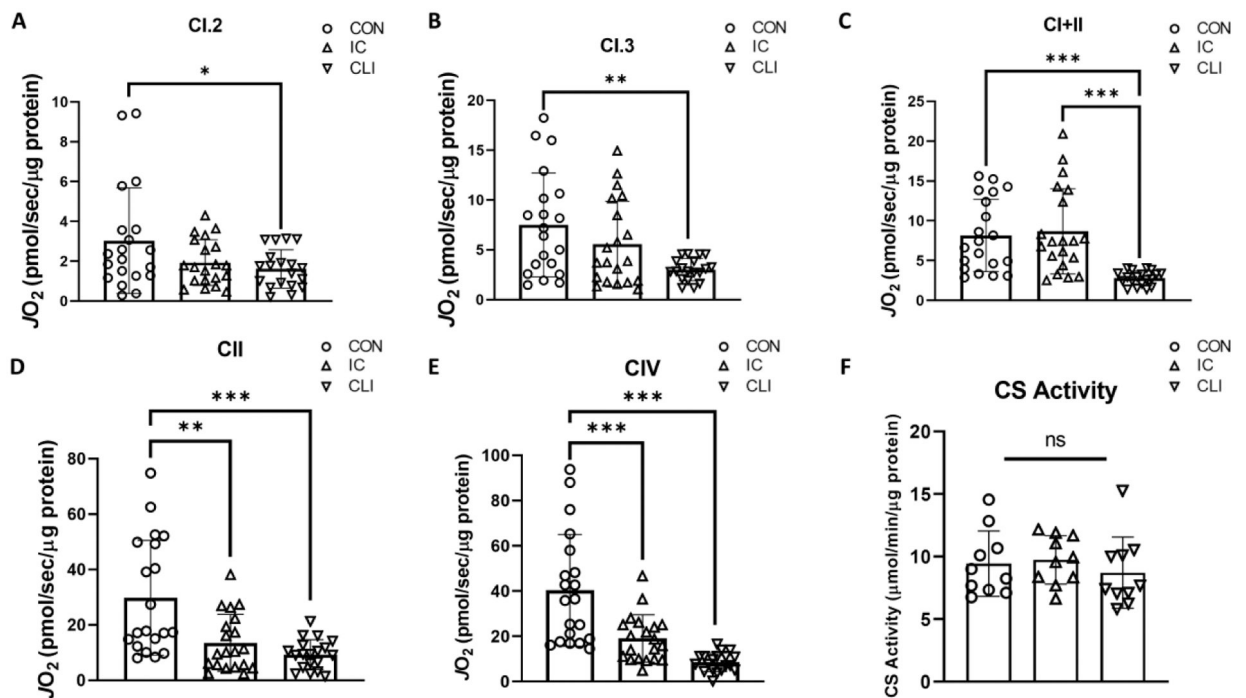
Figure 1. Skeletal muscle mitochondrial respiration is reduced in PAD patients.
Oxygen consumption rate (JO_2) in permeabilized muscle fibers from non-PAD control
(CON) patients (n=20), intermittent claudication (IC) patients (n=20), and critical limb
ischemia (CLI) patients (n=20). JO_2 measured during (**A**) Complex I, state 2 respiration
(CI.2), (**B**) Complex I, state 3 respiration (CI.3), **C,** combined Complex I and II respiration
(CI+II), (**D**) Complex II respiration (CII), and (**E**) Complex IV respiration (CIV). (**F**)
Mitochondrial content was assessed by citrate synthase (CS) activity. One-way ANCOVA
with post-hoc Bonferroni test used for analysis, ns represents no significant difference
between groups, ns represents no significant difference between groups, * represents $p<0.05$,
** represents $p<0.01$, and *** represents $p<0.001$.
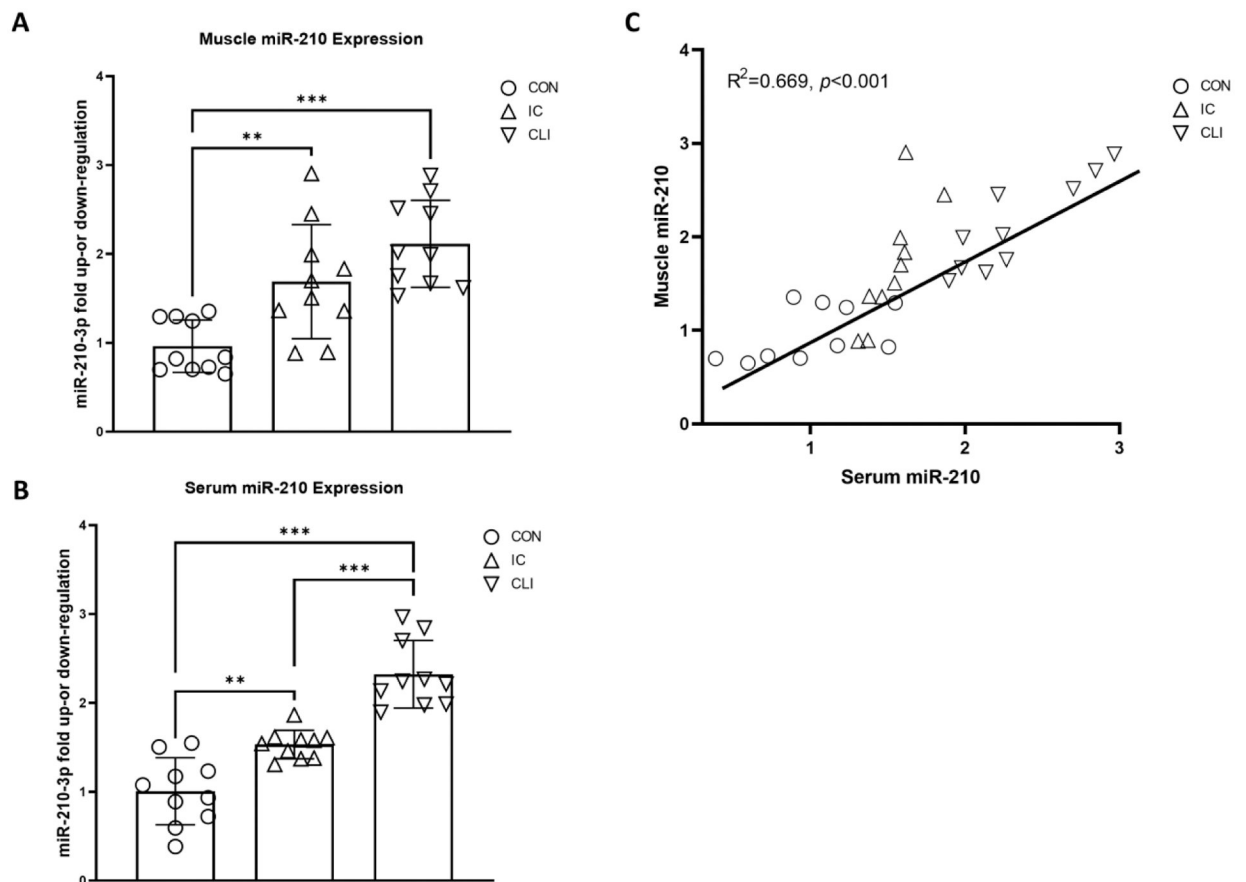
Figure 2. MiR-210 expression is elevated in PAD muscle.
(**A**) Relative miR-210 levels in gastrocnemius muscle of non-PAD control (CON) (n=10), intermittent claudication (IC) patients (n=10), and critical limb ischemia (CLI) patients (n=10) and (**B**) relative miR-210 levels in serum. One-way ANCOVA with post-hoc Bonferroni test used for analysis, ** represents $p<0.01$, and *** represents $p<0.001$. (**C**) Association between circulating levels of miR-210 and skeletal muscle levels of miR-210, correlation tested by Pearson correlation, coefficient of determination (R^2) and p-value for relationship shown.
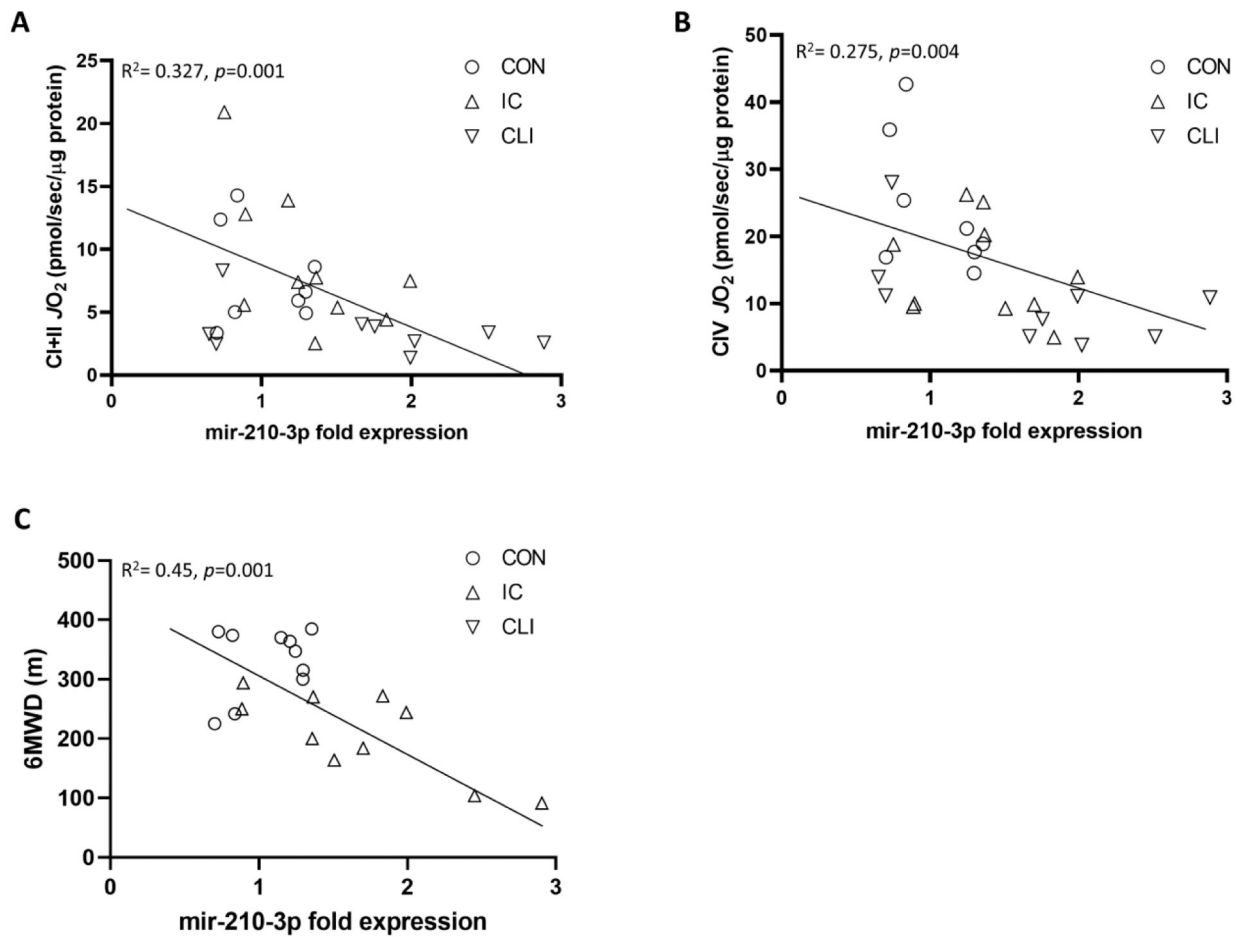
Figure 3. Skeletal muscle miR-210 expression is associated with mitochondrial respiration and walking performance.

(A) Association between combined Complex I and II (CI+II) respiration and skeletal muscle miR-210 relative expression in non-PAD control (CON), intermittent claudication patients, and critical limb ischemia (CLI) patients, **(B)** association between Complex IV (CIV) respiration and muscle miR-210 relative expression, and **(C)** association between 6-minute walk distance (6MWD) and muscle miR-210 relative expression. Correlations tested by Pearson correlation, coefficient of determination (R^2) and p-values for relationships shown.
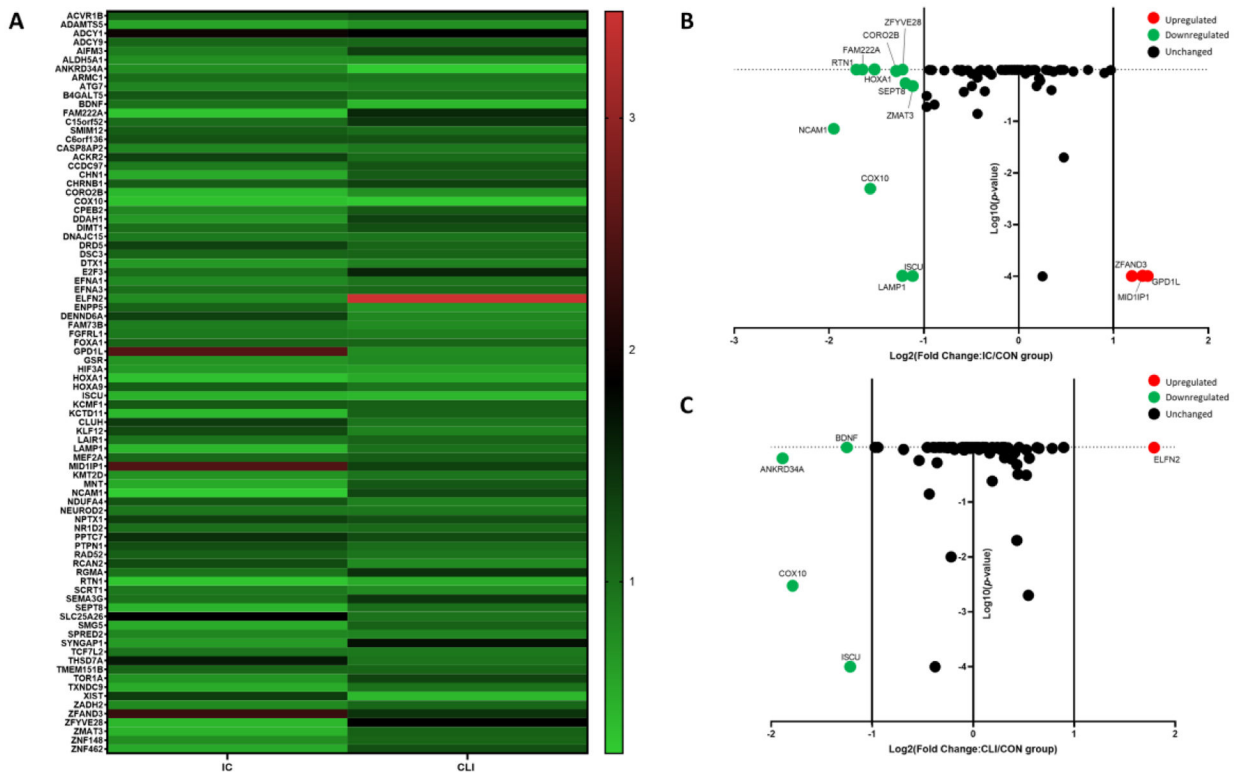
Figure 4. Skeletal muscle miR-210 target expression in PAD.

(A) Heatmap analysis of gastrocnemius tissue expression of miR-210 target genes, color legend represents calculated relative expression of intermittent claudication (IC) (n=6) and critical limb ischemia (CLI) patients (n=3) compared to non-PAD controls (CON) (n=3), **(B)** Volcano plot identifying significant gene expression changes in IC and **(C)** in CLI, by plotting the log2 of the fold changes in gene expression on the x-axis versus their statistical significance on the y-axis. The center vertical line indicates unchanged gene expression, while the two outer vertical lines indicate the selected fold regulation threshold. The horizontal line indicates the selected p-value threshold. Genes with data points in the far upper left (down-regulated) and far upper right (up-regulated) sections meet the selected fold regulation and p-value thresholds. By combining the fold change results with the p-value statistical test results, genes with both large and small expression changes that are statistically significant are easily visualized.
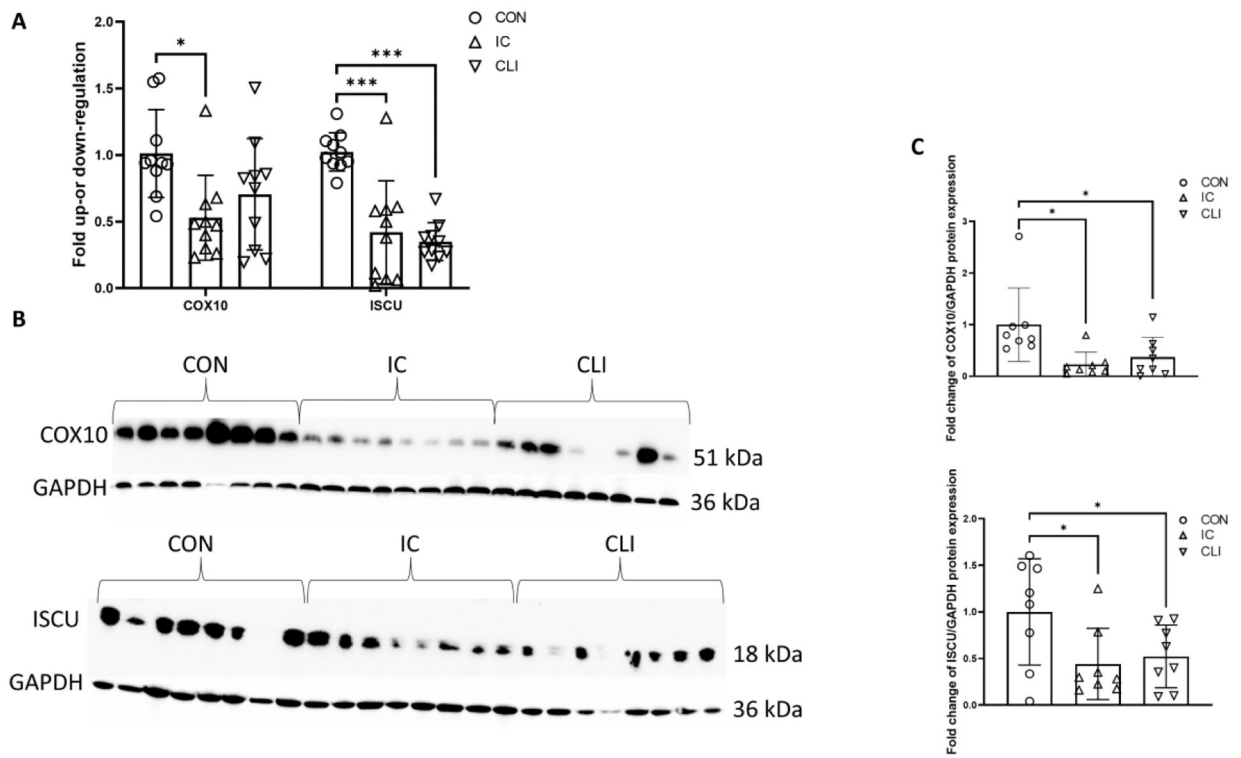
Figure 5. Skeletal muscle COX10 and ISCU expression are reduced in PAD.
(A) Relative fold change of mRNA expression detected by real-time PCR. COX10 and ISCU
gene expression measured in skeletal muscle homogenates of intermittent claudication (IC)
(n=10), critical limb ischemia (CLI) (n=10) patients, and non-PAD controls (CON) (n=10).
(B) Western blot of COX10 and ISCU, GAPDH used as loading control, **(C)** fold change
of COX10 and ISCU protein expression. One-way ANCOVA with post-hoc Bonferroni test
used for analyses, * represents $p<0.05$ and *** represents $p<0.001$.
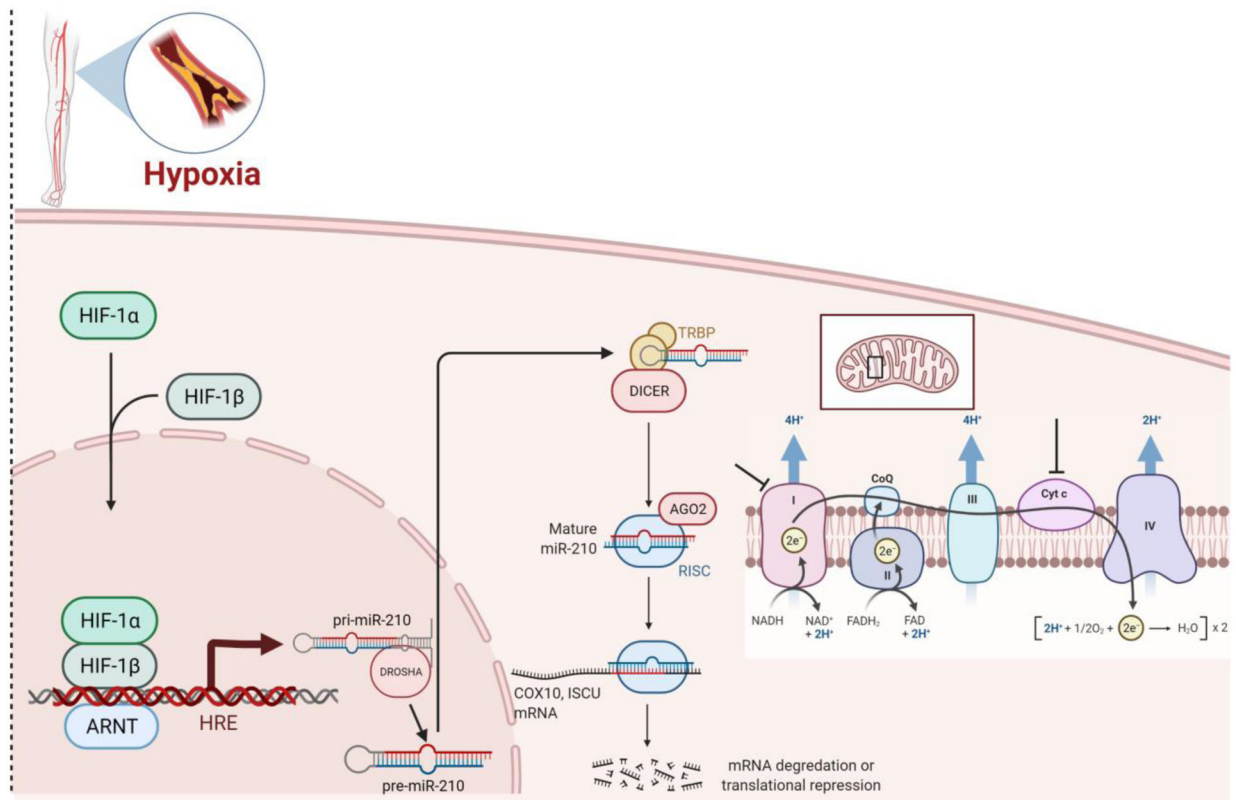
Figure 6. Potential mechanisms of miR-210 mediated mitochondrial dysfunction in PAD.
In ischemic conditions, hypoxia-inducible factor 1-alpha (HIF-1α) binds to the hypoxia
response element (HRE) on the miR-210 promoter, increasing the transcription of pri-
miR-210. After cleavage of excess base pairs by RNAse III Drosha, pre-miR-210 is exported
from the nucleus. RNAse III Dicer further cleaves the loop structure, separating the 2
strands of RNA, leaving a single stranded mature miR-210. The mature miR-210-RNA-
induced silencing complex (RISC) complexes can target and repress iron-sulfur cluster
scaffold homolog (ISCU) and cytochrome c oxidase assembly protein (COX10) genes.
The downregulation of these genes can lead to reduced activity of mitochondrial electron
transport chain Complex I and reduced expression of functional cytochrome c oxidase
protein.

Table 1.

Primers for Quantification of mRNAs by qPCR.

mRNA	5'————3'	Forward/Reverse	RefSeq[a] Number	Exon Location
COX10	AACATGAATAGGACAAAGAACAGAC	Forward	NM_001303	5–6
	AAGGTCAGAATGGCAACTCC	Reverse		
ISCU	GGAAGATTGTGGATGCTAGGT	Forward	NM_213595	4–5
	CTCCTTGGCGATATCTGTGTT	Reverse		
GAPDH [b]	ACATCGCTCAGACACCATG	Forward	NM_002046	2–3
	TGTAGTTGAGGTCAATGAAGGG	Reverse		
ACTB [b]	ACAGAGCCTCGCCTTTG	Forward	NM_001101	1–2
	CCTTGCACATGCCGGAG	Reverse		

[a] NCBI Reference Sequence database number

[b] Reference mRNA

Table 2.

Patient Clinical Characteristics

	Non-PAD Control (n=20)	Intermittent Claudication (IC) (n=20)	Critical limb ischemia (CLI) (n=20)	P-value[a]
Age (years)	54.67 ± 13.59	61.25 ± 6.18	62.40 ± 9.05	0.07
Sex (male/female)	4/16	12/8	12/8	0.01
Ethnicity (White/Hispanic/African American)	9/7/4	5/0/5	12/8/0	-
Ankle brachial index (ABI)	1.09 ± 0.01	0.79 ± 0.30	0.34 ± 0.16	<0.001
6-minute walk distance (6MWD) (m)	332.34 ± 86.53	184.54 ± 76.18	-	<0.001
Pain-free walking time (PFWT) (sec)	720 ± 47.20	53.25 ± 12.62	-	<0.001

[a]The values presented in the column "*p*-value" represent the overall difference between groups as determined by analysis of variance (ANOVA) for continuous variables or chi-square and Fisher exact tests for categorical variables.